

Original Article

Fatty acid extracts facilitate cutaneous wound healing through activating AKT, ERK, and TGF- β /Smad3 signaling and promoting angiogenesis

Junwei Zong^{1*}, Jun Jiang^{1*}, Peng Shi¹, Jing Liu², Weili Wang⁵, Bin Li², Tianda Zhao³, Taowen Pan⁴, Zhen Zhang¹, Liyan Bi⁶, Yunpeng Diao², Shouyu Wang¹

¹Department of Orthopedics, The First Affiliated Hospital of Dalian Medical University, Institute (College) of Integrative Medicine, Dalian Medical University, Dalian 116011, China; ²College of Pharmacy, ³Department of Scientific and Technology, ⁴Institute (College) Medicine, Dalian Medical University, Dalian 116044, China; ⁵School of Chemistry and Astbury Structure for Molecular Biology, University of Leeds, Leeds LS2 9JT, United Kingdom; ⁶Department of Geriatrics, The First Affiliated Hospital of Dalian Medical University, Dalian 116011, China. *Equal contributors.

Received September 27, 2019; Accepted January 10, 2020; Epub February 15, 2020; Published February 28, 2020

Abstract: Fatty acids (FAs) are potential therapeutic agents for cutaneous wound healing; however, the mechanisms underlying this effect have not been clearly defined. In this study, we extracted and characterized FAs from dried *Lucilia sericata* larvae and investigated the molecular basis by which FAs promote cutaneous wound healing. We first confirmed that FA sodium salts (FASSs) stimulated proliferation, migration, and tube formation of cultured *human umbilical vein endothelial cells* (HUVECs) in a dose-dependent manner. We then showed that FASSs promoted endothelial-to-mesenchymal transition (EndMT), which plays an important role in stabilizing the neovasculature during angiogenesis. Mechanistically, FASSs up-regulated the expression of angiogenesis-related growth factors, platelet-derived growth factor (PDGF), transforming growth factor- β 1 (TGF- β 1), and vascular endothelial growth factor A (VEGFA), and activated angiogenesis-related signaling pathways, AKT, ERK, and TGF- β /Smad3. In a rat acute cutaneous-wound model, FAs promoted wound healing. Following treatment, we further found that expression of anti-apoptosis-related factors (c-Myc and Bcl-2) was up-regulated and expression of apoptosis-related factors (p53 and Bad) was down-regulated. Our findings suggest that FAs can promote cutaneous wound healing by inducing angiogenesis, partly by activating AKT, ERK, and TGF- β /Smad3 signaling.

Keywords: Fatty acids, *Lucilia sericata* larvae, angiogenesis, signaling pathway

Introduction

Cutaneous wound healing involves highly coordinated multistep processes that precisely regulate the proliferation and migration of endothelial cells, deposition of the extracellular matrix (ECM), formation of new blood vessels (angiogenesis), and ultimately vascular remodeling. All wound healing events consist of a series of biochemical processes that are controlled by numerous nutrients [1-3]. When one or more of these processes are altered, wound healing is inefficient, characterized by delayed wound healing leading to a chronic wound. Multiple mechanisms underlie delayed wound healing, including inadequate production of growth factors and deficient angiogenesis [4, 5]. Given that chronic wounds pose heavy finan-

cial burdens to the affected individuals and families, it is imperative to identify treatments that may overcome delayed wound healing processes and/or facilitate wound healing.

Angiogenesis is an essential event during the cutaneous wound healing process. The newly generated blood vessels temporarily coordinate and spatially regulate other healing processes, such as the dynamic interaction between endothelial cells, proangiogenic factors, and ECM proteins [6]. Previous studies have shown that a number of proangiogenic factors including platelet-derived growth factor (PDGF) [7], transforming growth factor- β 1 (TGF- β 1) [8], and vascular endothelial growth factor A (VEGFA) [9, 10] activate protein kinase signaling pathways, such as phosphatidylinositol 3 kinase (PI3K)/v-

Fatty acid extracts promote wound healing

Akt [11], mitogen-activated protein kinase (MAPK) (i.e. p38 MAPK pathway) [12], extracellular signal-regulated protein kinase 1 and 2 (ERK1/2) [13], and transforming growth factor beta (TGF- β)/Smad [14]. These proangiogenic factors promote cell proliferation and migration, as well as angiogenesis during the progression of wound healing [11, 14, 15]. In contrast, angiogenesis is supported by other cellular events that may stabilize the neovasculature [16-21]. One such event is endothelium to mesenchyme transition (EndMT) [22]. During EndMT, the surrounding endothelial cells acquire a mesenchymal phenotype, which is characterized by the loss of endothelial markers and a subsequent gain of mesenchymal markers. Cells derived from EndMT exhibit characteristics that resemble the function of fibroblasts in damaged tissue, thus contributing to both tissue remodeling and neovasculature stabilization [22].

Since restoring injured dermal tissues requires energy, natural remedies that are rich in proteins, such as fatty acids (FAs), have been used to promote the wound healing process. FAs are an essential component of cell membranes and the key source of energy production that facilitates the metabolic processes involved in cutaneous wound healing [23]. Studies have also shown that FAs participate in biologic activities such as angiogenesis [24, 25]. Our previous work showed that FAs, derived from *Lucilia sericata* larvae, enhanced the cutaneous wound healing process by promoting angiogenesis [26]. However, it remains unknown whether the signaling pathways described above are involved in FA-mediated cell proliferation, migration, and angiogenesis.

In the present study, we extracted and characterized FA sodium salts (FASSs) from *L. sericata* larvae and investigated their effect on endothelial cell proliferation, migration, and tube formation of cultured *human umbilical vein endothelial cells* (HUVECs). We also determined the wound healing- and angiogenesis-promoting effects of FAs in a rat acute cutaneous wound model.

Materials and methods

Antibodies and reagents

Antibodies against α -smooth muscle acting (α -SMA), phosphorylated (p)-AKT1 (S473), p-ER-

K1/2 (T202, T185), p-p38 (T180, Y182), and p-Smad3 (S423, S425) were purchased from Abcam (Cambridge, MA, USA). Antibodies against CD31, Ki-67, AKT1, ERK1/2, p38, TGF- β , and GAPDH were purchased from Proteintech Group (Chicago, USA). Smad3 antibody was purchased from Arigo Biolaboratories (Taiwan, China). Alexa Fluor 594-conjugated secondary antibodies were purchased from Invitrogen (CA, USA). Chemicals SIS3, AZD5363, SCH772984, and SB203580 were purchased from MedChem Express (NJ, USA).

FA extraction and purification

The dried bodies of *L. sericata* were purchased from a traditional Chinese medicine market in Boluo Country, Huizhou, Guangzhou Province. The *L. sericata* bodies were ground into powder, followed by ethyl acetate extraction using 10 g of powder in 150 mL of 95% ethyl acetate in a Fat Analyzer (BYSXY-06, BY, China) in a 77 \pm 2 $^{\circ}$ C water bath for approximately 2 h. The filtered ethyl acetate extraction was then transferred to a rotary evaporator, and the solvent was ultimately evaporated. The FA extracts were then purified through the following steps: 1 mg of FA was dissolved in 4 mL of benzene:petroleum ether (1:1 volume:volume) and 4 mL of NaOH-methyl alcohol (0.2 mol/L). After intense vortexing, the mixture was heated in a water bath at 70 \pm 1 $^{\circ}$ C for 30 min, followed by the addition of 10 mL of deionized water. The supernatant was transferred into a new sterile 10-mL tube and dried under nitrogen. The samples were stored at 4 $^{\circ}$ C for future studies.

Qualitative analysis of FA extracts

Purified FAs were dissolved in 200 μ L of ethyl acetate for GC-MS analysis. GC-MS analysis was performed using a GC-MS-QP2020 (Shimadzu, Japan) under the following conditions. A Rxi-5Sil MS capillary column (30 m \times 0.25 mm \times 0.25 μ m) was programmed with the following oven temperatures: initial temperature at 60 $^{\circ}$ C for 1 min; 5 $^{\circ}$ C/min up to 170 $^{\circ}$ C; 5 min at 170 $^{\circ}$ C; 5 $^{\circ}$ C/min up to 230 $^{\circ}$ C; and 5 min at 230 $^{\circ}$ C. The injection temperature was 250 $^{\circ}$ C, the injection mode was split (split ratio =10:1), the injection volume was 1 μ L, and the carrier gas was helium. The MS conditions were set as follows: 70 eV electron impact (EI) ionization, 230 $^{\circ}$ C ion source temperature, 250 $^{\circ}$ C interface temperature, and acquisition mode scanning (m/z 45-600).

Fatty acid extracts promote wound healing

Preparation of FASS solution

To improve the hydrophilicity of the FA extracts, approximately 0.1 g of purified FAs was saponified in 1 mL of a 0.1 mol/L NaOH solution, fully vortexed, and heated in a water bath at $70\pm 1^\circ\text{C}$ for 30 min. Thereafter, a 100 mg/mL FASS solution was filtered through a 0.22-mm filter membrane at appropriate concentrations, and the solution was stored at -20°C until further use. After serial dilution in the full cell culture medium, the FASS pH was neutral and did not affect cell activity.

Cell culture

HUVECs were obtained from American Type Culture Collection (ATCC, Rockville, MD, USA) and were cultured in Dulbecco's modified Eagle's medium (DMEM, Gibco, Carlsbad, CA, USA) containing 10% fetal bovine serum (FBS; Biological Industries, Israel) supplemented with 1% penicillin-streptomycin in a humidified atmosphere containing 5% CO_2 at 37°C .

Cell viability assay

Cell viability was determined using the Cell Counting Kit-8 (CCK-8, Dojindo, Kumamoto, Japan). Briefly, HUVECs were seeded in 96-well plates at 2×10^3 cells per well and incubated at 37°C for 24 h. Fresh medium with different concentrations of FASSs was added into the culture medium and incubated with cells for 24 h. Subsequently, the CCK-8 reagent was added according to the manufacturer's instructions. Cytotoxicity was calculated as the relative viability (%), with 100% representing no FASSs in the culture medium (0 ng/mL FASS, control group). At least four independent experiments were performed for each group.

Cell proliferation assay

Cell proliferation was determined by counting cells using a hemocytometer. Briefly, 5×10^3 HUVECs were seeded in 24-well plates and incubated at 37°C for 12 h. Cells were harvested after 24 h of treatment with different concentrations (0, 0.1, 1, and 50 ng/mL) of FASSs. Equal volumes of media were added to the cells. Approximately 10 μL of the cell suspension was placed at the edge of the cover-slip of a Burker chamber, and the hemocytometer grid was visualized under an optical microscope

(Olympus CKX41, Olympus, Japan). To calculate the number of viable cells per field, the average number of cells in one large square was multiplied by the dilution factor and then by 10^4 . At least four independent experiments were performed for each group.

Scratch assay

A scratch assay was performed as previously reported [27]. Briefly, HUVECs were cultured in 12-well plates with 2 mL of DMEM containing 10% FBS, and a scratch wound was generated on the confluent HUVECs. After removal of culture medium and washing with phosphate buffered saline (PBS), the cells were incubated with different concentrations (0, 0.1, 1, and 50 ng/mL) of FASSs at 37°C for 24 h. Images were acquired with an inverted microscope (Nexcope NIB410, USA) at 0, 12, and 24 h and were further quantified using ImageJ software (NIH, Bethesda, MD, USA). At least four independent experiments were performed for each group.

Transwell assays

HUVEC migration activity was determined using 24-well Transwell chambers (6.5-mm diameter, 8.0- μm pore size; Corning Incorporated, Corning, NY, USA). In brief, HUVECs (2×10^4 cells) were suspended in 200 μL of serum-free medium and then added to the upper chamber. In each lower chamber, 1 mL of serum-free medium containing different concentrations of FASSs (0, 0.1, 1, and 50 ng/mL) was added. Cells on the upper layer of the membrane were removed with swabs after incubation at 37°C for 24 h. Cells that migrated through the membrane were fixed with 4% paraformaldehyde and stained with crystal violet. Stained cells were observed under a microscope (Nexcope NIB410, USA), and at least six fields of view were observed for each group.

Capillary tube formation assay

Each well of a 96-well plate was pre-coated with 50 μL of Matrigel (Becton Dickinson Labware, Franklin Lakes, NJ, USA) at 37°C for 30 min. HUVECs were added to the top of the gel at a density of 3×10^4 cells per well in the presence of different concentrations of FASSs (0, 0.1, 1, and 50 ng/mL), and incubated at 37°C for another 6-8 h. Images were acquired under a microscope (Nexcope NIB410, USA).

Fatty acid extracts promote wound healing

Length, branch length, and node number were measured for each tube and analyzed using ImageJ software. At least six fields of view were observed for each group.

ELISA

At 24 h after FASSs administration (0, 0.1, 1, and 50 ng/mL), HUVEC supernatants were collected, and the amount of secreted PDGF-BB and VEGFA was quantified using a human PDGF-BB ELISA kit (Westang, Shanghai, China) and a human VEGFA ELISA kit (Proteintech, Chicago, USA), respectively, according to the manufacturer's instructions. Protein concentrations were determined based on standard curves. At least four independent experiments were performed for each group.

Immunofluorescence

HUVECs were washed with PBS, fixed in 4% paraformaldehyde for 20 min, permeabilized with 0.3% Triton X-100 for 3 min, blocked with 5% goat serum at 37°C for 30 min, and incubated with the following primary antibodies at 4°C overnight: p-Smad3 (1:50) or α -SMA (1:100). Thereafter, cells were incubated in the dark with the corresponding fluorescent dye-conjugated secondary antibodies (Alexa Fluor 594; 1:200; Invitrogen) at 37°C for 90 min and then with DAPI for 20 min. Images were acquired sequentially with the fluorescence microscope (Olympus IX73, Olympus, Japan). At least six randomly selected fields per group were observed.

Western blot assay

Cells were collected, washed, and lysed in RIPA buffer (10 mM Tris (pH 7.4), 150 mM NaCl, 1 mM EGTA, 0.1% SDS, 1 mM NaF, 1 mM Na_3VO_4) containing protease inhibitors (1 mM phenylmethylsulfonyl fluoride, 1 mg/mL aprotinin, and 1 mg/mL leupeptin). The protein concentration of each sample was determined using a bicinchoninic acid (BCA) protein assay kit (Thermo Scientific, Fremont, CA, USA). Protein samples (60 μg) were separated in a 10% SDS-polyacrylamide gel and then transferred onto polyvinylidene fluoride (PVDF) membranes. The membranes were blocked with 5% skim milk for 2 h, incubated with the primary and horseradish peroxidase (HRP)-conjugated secondary antibodies, and visualized using an enhanced

chemiluminescence (ECL) reagent and a ChemiDoc system (Bio-Rad, Hercules, CA, USA). The densities of specific protein bands were quantitated using a Molecular Dynamics densitometer with MD Image Quant software (GE Healthcare Life Sciences). The following primary antibodies were used in the experiments: CD31 (1:500), α -SMA (1:500), AKT1 (1:1,000), ERK1/2 (1:1,000), p38 (1:1,000), TGF- β (1:500), Smad3 (1:1,000), p-AKT1 (1:500), p-ERK1/2 (1:500), p-p38 (1:500), p-Smad3 (1:500), and GAPDH (1:2,000). The secondary antibodies were HRP-conjugated goat anti-rabbit antibodies (1:2,000). To further confirm that these signaling pathways were activated by FASSs, the inhibitors SIS3 (0.5 μM , a Smad3 inhibitor), AZD5363 (10 nM, an AKT1 inhibitor), SCH772984 (0.5 μM , an ERK1/2 inhibitor), and SB203580 (0.5 μM , a p38 MAPK inhibitor) were used in the scratch and Transwell assays. At least four independent experiments were performed for each group.

Real-time quantitative PCR (RT-qPCR)

Total RNA was isolated from HUVECs using TransZol. cDNA was synthesized from 1 μg of total RNA with an All-in-One First-Strand cDNA Synthesis kit. The relative mRNA expression was quantified using RT-qPCR with Top Green qPCR SuperMix (all kits were purchased from Transgen, Beijing, China). RT-qPCR was performed on an ABI Prism 7500 device (Applied Biosystems, USA), and the primer sequences used in this study are listed in **Table 1**. Each experiment was performed in triplicate. The relative gene expression was normalized to GAPDH and calculated using ABI Prism 7500 v.2.0.6 software (Applied Biosystems, USA) with the $2^{-\Delta\Delta\text{Ct}}$ method. At least four independent experiments were performed for each group.

Generation of rat skin wound model and treatment

Animal procedures complied with the guidelines of the Association for the Assessment and Accreditation of Laboratory Animal Care International and were approved by the Animal Research Committee of Dalian Medical University. A rat model of acute cutaneous wound injury was established as described previously [27]. Briefly, rats were anaesthetized with 12 mg/kg xylazine via intraperitoneal

Fatty acid extracts promote wound healing

Table 1. Sequences of RT-qPCR primers

Primers	Sequences	Length (bp)
α-SMA (human)	F: 5'-GACGAAGCACAGACAA-3' R: 5'-GTGGGATGCTCTTCAG-3'	150
CD31 (human)	F: 5'-CACTGAAGACGTCGAAT-3' R: 5'-CCAGACTCCACCACCTTACT-3'	150
VEGFA (human)	F: 5'-GTACCCTGATGAGATCGAGTA-3' R: 5'-TGAGGTTTGATCCGCATA-3'	151
TGF-β (human)	F: 5'-CAGAGTGGTTATCTTTTGA-3' R: 5'-TAGTGAACCCGTTGATGT-3'	150
PDGF (human)	F: 5'-GCACCAACGCCAATCTCT-3' R: 5'-ACCGTGGCCTTCTTAAAGATTG-3'	171
GAPDH (human)	F: 5'-GCACCGTCAAGGCTGAGAAC-3' R: 5'-TGGTGAAGACGCCAGTGGA-3'	137
c-Myc (Rat)	F: 5'-ACCCCTCCACAAGGAA-3' R: 5'-ACGTTGTGTGCCCTCTT-3'	150
Bcl-2 (Rat)	F: 5'-CGGTGGTGGAGGAAGTCTTC-3' R: 5'-TGTGCAGATGCCGGTTCA-3'	165
Bad (Rat)	F: 5'-TGAGGAAGATGAAGGATGGA-3' R: 5'-CGAGGAAGTCCCTTGAAGGAA-3'	150
p53 (Rat)	F: 5'-AGAGGAAGAAAATTCGCAAA-3' R: 5'-CCACGGATCTTAAGGGTGAATAT-3'	150
GAPDH (Rat)	F: 5'-GGCACAGTCAAGGCTGAGAATG-3' R: 5'-ATGGTGGTGAAGACGCCAGTA-3'	142

injection. A 1.5-cm diameter round open wound down to the muscle fascia was generated on the back by removing the skin layer (epidermis and dermis). A total of 24 Sprague-Dawley rats (10 weeks old, 230-250 g) were randomly divided into three groups (8 per group): an experimental group, in which the animals were treated with 0.1 g of FAs per wound; a negative group, in which the animals were treated with 0.1 g of Vaseline ointment per wound; and a positive group, in which the animals were treated with 0.1 g of JingWanHong ointment (a traditional Chinese patented medicine to treat wounds; Beijing Tongrentang Pharmacy, China). Four rats were sacrificed from each group at day 5 post-wounding, and the tissues were harvested and stored at -80°C for future study. All treatments were applied topically twice a day until the wounds healed completely. Four independent experiments were performed for each group.

Digital transparency wound area measurement

The wound area was measured using a high throughput transparency tracing sheet as

described previously [28]. Briefly, the wound margins of each animal at different observation times (1, 3, 5, 7, 9, 11, and 13 days post-wounding) were traced with a transparency model sheet and scanned with an HP Laser Jet M1005MFP. The images were saved in JPG form and were opened with Adobe Photoshop CS6 (Adobe Systems Incorporated, San Jose, CA). The pixel values of each individual wound were calculated, and the data were recorded in an Excel format. The real area of the individual wound was normalized to a standard unit and calculated by three independent researchers.

Hematoxylin and eosin (H/E) staining

Tissues were fixed in 4% paraformaldehyde (pH 7.4) and gradually dehydrated, embedded in paraffin, cut into 4-μm sections, stained with H/E, and observed under a light microscope (Nexcope NIB410, USA). ImageJ software was used for morphometric analyses, and the microvascular density was assessed. At least six randomly selected fields of each group were scored.

Immunohistochemistry (IHC)

IHC was conducted according to the manufacturer's instructions. Briefly, skin tissues were fixed in 4% paraformaldehyde and embedded in paraffin. Paraffin sections (4-μm thickness) of the tissue samples were prepared and incubated with the primary antibodies against Ki-67 (1:200) at 4°C overnight, followed by another incubation with a peroxidase-labelled polymer conjugated to goat anti-rabbit immunoglobulins for analysis via light microscopy (Nexcope NIB410, USA). The images were analyzed using IPwin32 software. At least six randomly selected fields per group were scored.

Statistical analysis

Data are expressed as the mean ± the standard error of the means (SEM) of at least three independent experiments. Statistical analyses

Fatty acid extracts promote wound healing

Table 2. Components of FA extracts from dried *Lucilia sericata* larvae

No.	Retention time (min)	Compound	Molecular formula	Relative content (%)
1	25.934	Myristic acid	C ₁₄ H ₂₈ O ₂	2.78
2	28.546	13-methyltetradecanoic acid	C ₁₅ H ₃₀ O ₂	0.83
3	29.629	Pentadecanoic acid	C ₁₅ H ₃₀ O ₂	0.42
4	31.802	7,10-Hexadecadienoic acid	C ₁₆ H ₂₈ O ₂	1.57
5	32.114	Palmitoleic acid	C ₁₆ H ₃₀ O ₂	3.48
6	32.373	(9E)-9-Hexadecenoic acid	C ₁₆ H ₃₀ O ₂	20.89
7	33.006	Palmitate acid	C ₁₆ H ₃₂ O ₂	14.42
8	34.860	Hexadecanoic acid, 14-methyl-	C ₁₇ H ₃₄ O ₂	0.52
9	35.170	cis-9-Hexadecenoic acid	C ₁₆ H ₃₀ O ₂	0.64
10	37.364	Linoleic acid	C ₁₈ H ₃₂ O ₂	24.52
11	37.553	Elaidic acid	C ₁₈ H ₃₄ O ₂	26.21
12	38.051	Octadecanoic acid	C ₁₈ H ₃₆ O ₂	3.72

were performed using SPSS 19.0 (SPSS, Inc., Chicago, IL, USA) or Prism 5.0 (GraphPad Software, La Jolla, CA, USA). Quantitative data were analyzed using a two-tailed Student's t-test for two group comparison, or one-way analysis of variance (ANOVA) followed by Dunnett's post hoc test for multiple group comparisons. Differences were considered statistically significant at $P < 0.05$ and highly significant at $P < 0.01$.

Results

Determination of FA components using GC-MS

We first characterized the components of FAs purified from dried *L. sericata* larvae using GC-MS, and the percent of each component was determined based on the peak area normalization method. The twelve major types of identified FAs are shown in **Table 2**. The percentages of saturated fatty acids (SFAs), mono-unsaturated fatty acids (MUFAs), and polyunsaturated fatty acids (PUFAs) were 22.69%, 51.22%, and 26.09%, respectively.

FASSs promote proliferation and migration of HUVECs

To determine the effects of FASSs on endothelial cell growth, we evaluated the viability of HUVECs treated with various FASSs concentrations for 24 h using the CCK-8 assay. We found that concentrations between 0.1 and 50 ng/mL FASSs treatment promoted cell growth (**Figure 1A**). Based on this observation, we

chose the concentrations of 0.1, 1, and 50 ng/mL for the subsequent studies. The FASSs effects were further confirmed by a cell count assay (**Figure 1B**), which showed that FASSs promoted cell proliferation in a dose-dependent manner. We next examined the effects of FASSs on endothelial cell migration, which plays a crucial role in angiogenesis [29]. HUVECs were incubated with different FASS concentrations (0, 0.1, 1, and 50 ng/mL) for 24 h, followed by the wound healing and Transwell assays. As shown in **Figure 1C, 1D**, FASS

treatments increased the HUVEC migratory capacity in a dose-dependent manner compared to the control group.

FASSs promote angiogenesis of HUVECs

We next evaluated endothelial cell formation of capillary-like structures in response to FASS stimulation. After treatment for 6 h, we analyzed tube length, branch length, and node number, and revealed that FASS-treated HUVECs presented a significantly increased ability to form new tube structures compared to untreated HUVECs (**Figure 2A**). To further explore how FASSs enhanced angiogenesis, we measured the expression levels and concentrations of two pro-angiogenic cytokines, VEGFA and PDGF-BB, in the cells and culture medium obtained from control and treatment groups using RT-qPCR and ELISA. As shown in **Figure 2B**, FASSs significantly increased the mRNA expression and release of both VEGFA and PDGF-BB

FASSs promote neovasculature stabilization and maturation

EndMT plays an important role in stabilizing the neovasculature during vasculogenesis and angiogenesis [22]. Therefore, we investigated the expression of α -SMA, an important protein marker of vasculogenesis and angiogenesis, whose up-regulation contributes to neovasculature stabilization. FASSs dose-dependently increased α -SMA expression compared to the control group (**Figure 2C, 2D**). CD31 is a widely

Fatty acid extracts promote wound healing

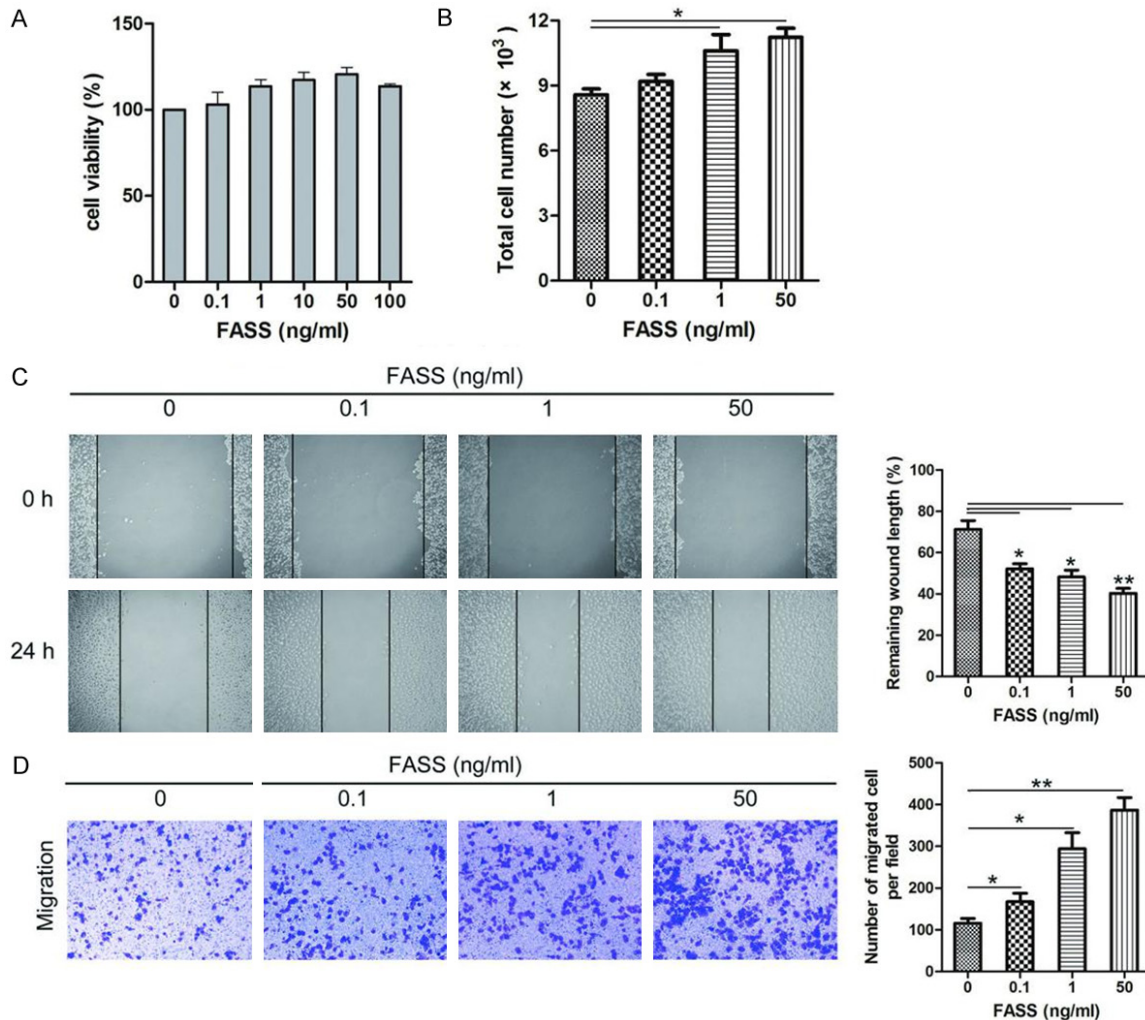


Figure 1. FASSs promoted HUVEC proliferation and migration in a dose-dependent manner. A. CCK-8 assay for evaluating HUVEC viability. B. FASSs augmented HUVEC proliferation as determined using a hemocytometer. C, D. Scratch assay and Transwell assay on HUVECs. FASSs showed notable increased migratory capacity in a dose-dependent manner compared to the control group. * $P < 0.05$, ** $P < 0.01$.

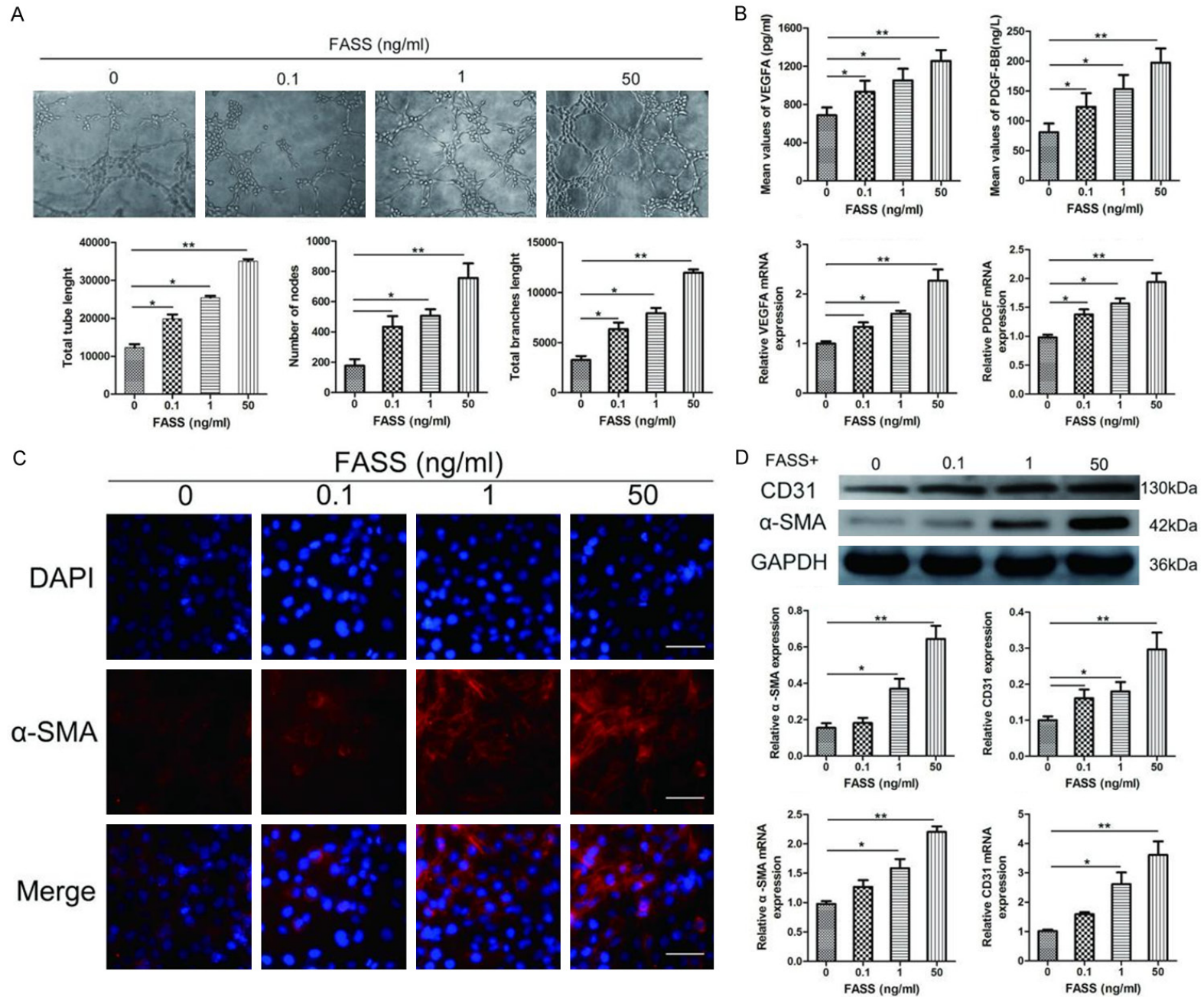
used endothelial cell marker of newly formed blood vessels [30]. We measured CD31 expression in the control and FASSs-treated HUVECs. As shown in **Figure 2D**, FASSs significantly augmented CE31 mRNA levels and protein expression in a dose-dependent manner compared to the control group. These observations suggest that FASSs increase the expression of both CD31 and α -SMA, both of which are indicators of maturing blood vessels [31].

FASSs activate TGF- β /Smad3 signaling in HUVECs

The TGF- β superfamily includes autocrine signaling molecules that can induce EndMT [32].

Immunofluorescence, RT-qPCR, and Western blot analyses were used to assess the effects of FASSs on TGF- β /Smad3 activity. As shown in **Figure 3A**, FASSs induced Smad3 phosphorylation (p-Smad3) in a dose-dependent manner. Correspondingly, FASSs treatment promoted nuclear translocation of p-Smad3. Consistent with the above observation, FASSs dose-dependently upregulated the expression of TGF- β , an upstream regulator of Smad3, at both mRNA and protein levels. The implication of TGF- β /Smad3 signaling in FASSs-mediated angiogenesis was further supported using the specific Smad3 inhibitor SIS3, which partially suppressed FASSs-induced cell proliferation and migration (**Figure 3C**). Thus, our data sug-

Fatty acid extracts promote wound healing



Fatty acid extracts promote wound healing

Figure 2. FASSs promoted HUVEC tube formation and stabilized the neovasculature. A. FASSs promoted HUVEC tube length, node number, and branch length of the tubes in a dose-dependent manner. Magnification, 100 \times . B. FASSs promoted the release of proangiogenic factors from HUVECs in a dose-dependent manner. ELISA and RT-qPCR were performed on control (0) and FASSs-treated HUVECs. C. Representative immunofluorescence images of α -SMA expression in HUVECs after treatment with FASSs. Magnification, 400 \times . D. Western blot and RT-qPCR revealed that FASSs dose-dependently significantly increased expression of α -SMA and CD31 in HUVECs. * $P < 0.05$, ** $P < 0.01$.

gest that FASSs activate TGF- β /Smad3, which plays a role in FASSs-mediated proliferation and migration of HUVECs.

FASSs activate AKT1 and ERK1/2 signaling in HUVECs

As previous studies have shown that PI3K/AKT1, ERK1/2, and p38 MAPK regulate cell proliferation, migration, and angiogenesis during wound healing [11, 12, 14, 15], we next determined the changes in the activity of these signaling pathways in the control and FASSs-treated HUVECs using Western blot analysis. We found that FASSs treatment induced the phosphorylation levels of AKT1, ERK1/2, and p38 MAPK in a dose-dependent manner (**Figure 4A-C**). To further confirm the effects of FASSs on these signaling pathways, we employed a specific inhibitor of each of these three pathways, AZD5363 (AKT1 inhibitor), SCH772984 (ERK1/2 inhibitor), and SB203580 (p38 MAPK inhibitor). We found that the AKT1 and ERK1/2 inhibitors, but not the p38 MAPK inhibitor, attenuated the effects of FASSs, indicating that the AKT1 and ERK1/2 pathways, but not the p38 MAPK pathway, were involved in the FASS-induced biological effects in HUVECs. We also observed that simultaneous application of these inhibitors completely abolished the effects of FASSs on the activation of these molecules (**Figure 4D**). Thus, our data indicate that FASSs induce activation of the AKT1 and ERK1/2 pathways in HUVECs.

FAs accelerate cutaneous wound healing via cell proliferation in vivo

We next evaluated the effects and related mechanisms of FAs in an acute cutaneous wound model *in vivo*. The healing rates of cutaneous wounds following different treatments were evaluated sequentially using a transparency tracing digital calculation method [28]. A total of 84 traces, which are shown as one transparency model sheet (**Figure 5A**), were collected from twelve open cutaneous wounds at seven time points (days 1, 3, 5, 7, 9, 11, and

13) in this study. As shown in **Figure 5B**, the average wound healing rates were higher in the FA and positive rat groups than in the control group, especially at days 5, 7, 9, and 11. The wound tissues of the three experimental groups were further histologically analyzed using H/E staining. As shown in **Figure 5C** (arrows), the number of microvascular structures was greater in the FA and positive groups than in the control group. We also examined cell proliferation in the wound region by staining with Ki-67, which is a well-recognized marker of proliferating cells [33]. The number of Ki-67-positive cells in the wound tissues of the FA and positive groups was significantly higher compared to the control group (**Figure 5D**). To understand the molecular basis underlying the increased proliferation mediated by FAs, we evaluated the expression of proliferation-related genes *c-Myc* and *Bcl-2*, and apoptosis-related genes *Bad* and *p53*, in the wound tissues of these three groups using RT-qPCR. We found that FA treatment markedly up-regulated the expression of *c-Myc* and *Bcl-2*, which coincided with decreased expression of *Bad* and *p53* (**Figure 5E**). Therefore, our data suggest that FAs accelerate cutaneous wound healing by promoting cell proliferation in an *in vivo* rat model.

Discussion

Angiogenesis is a complex process that controls the formation of new blood vessels and is essential for cutaneous wound healing [31]. FAs, a natural product, have been reported to have various biological activities, including promoting angiogenesis and cutaneous wound healing [24, 25]. However, the mechanisms underlying these activities are not fully understood. Our findings indicate that FASSs promote HUVEC proliferation and migration, which play a critical role in angiogenesis by stimulating AKT1, ERK1/2, and TGF- β 1/Smad3 signaling and increasing expression of CD31 and α -SMA to stabilize the neovasculature. The underlying mechanisms involve increased levels of proangiogenic cytokines, such as VEGFA, PDGF, and TGF- β 1 [7-10], which

Fatty acid extracts promote wound healing

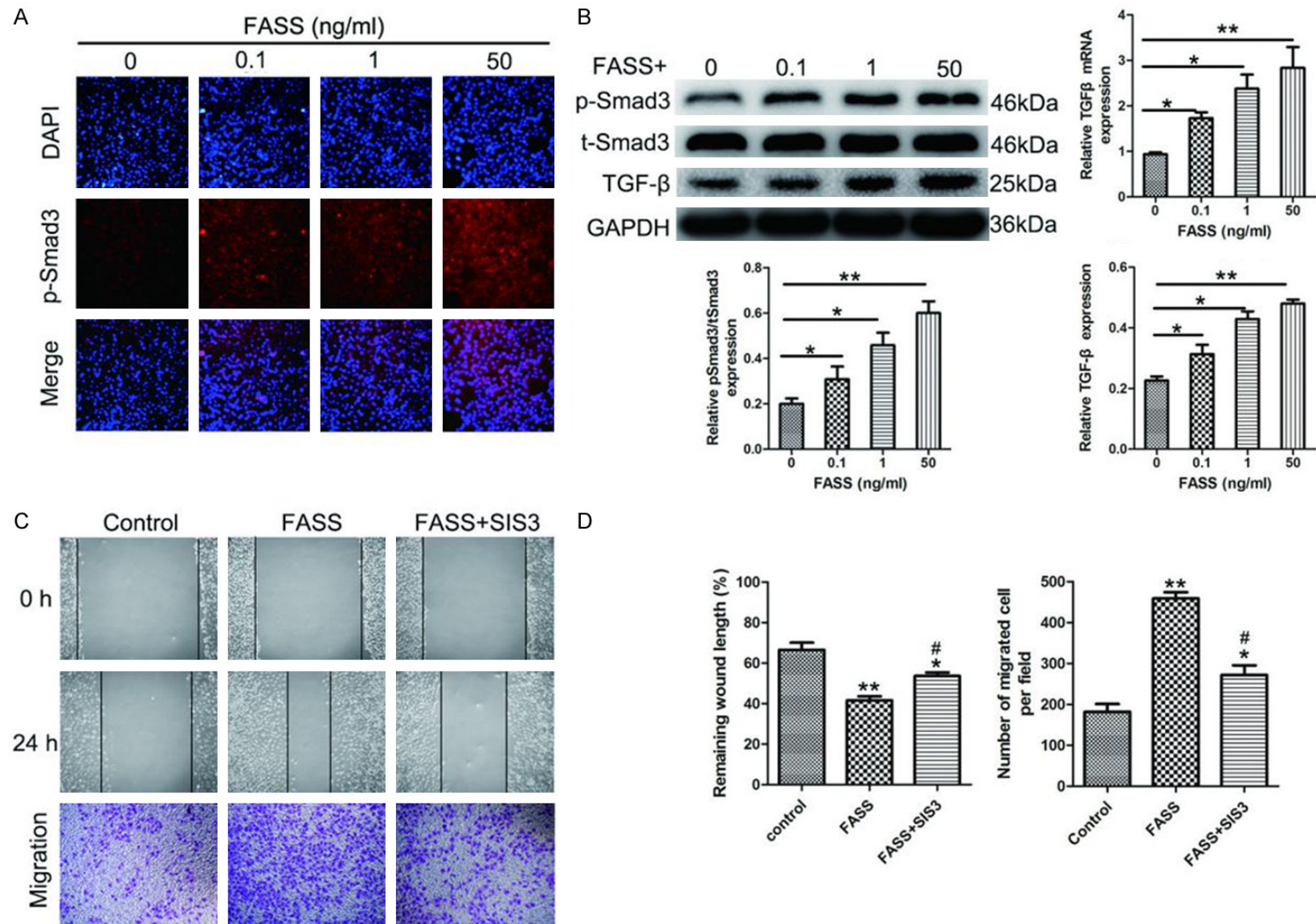
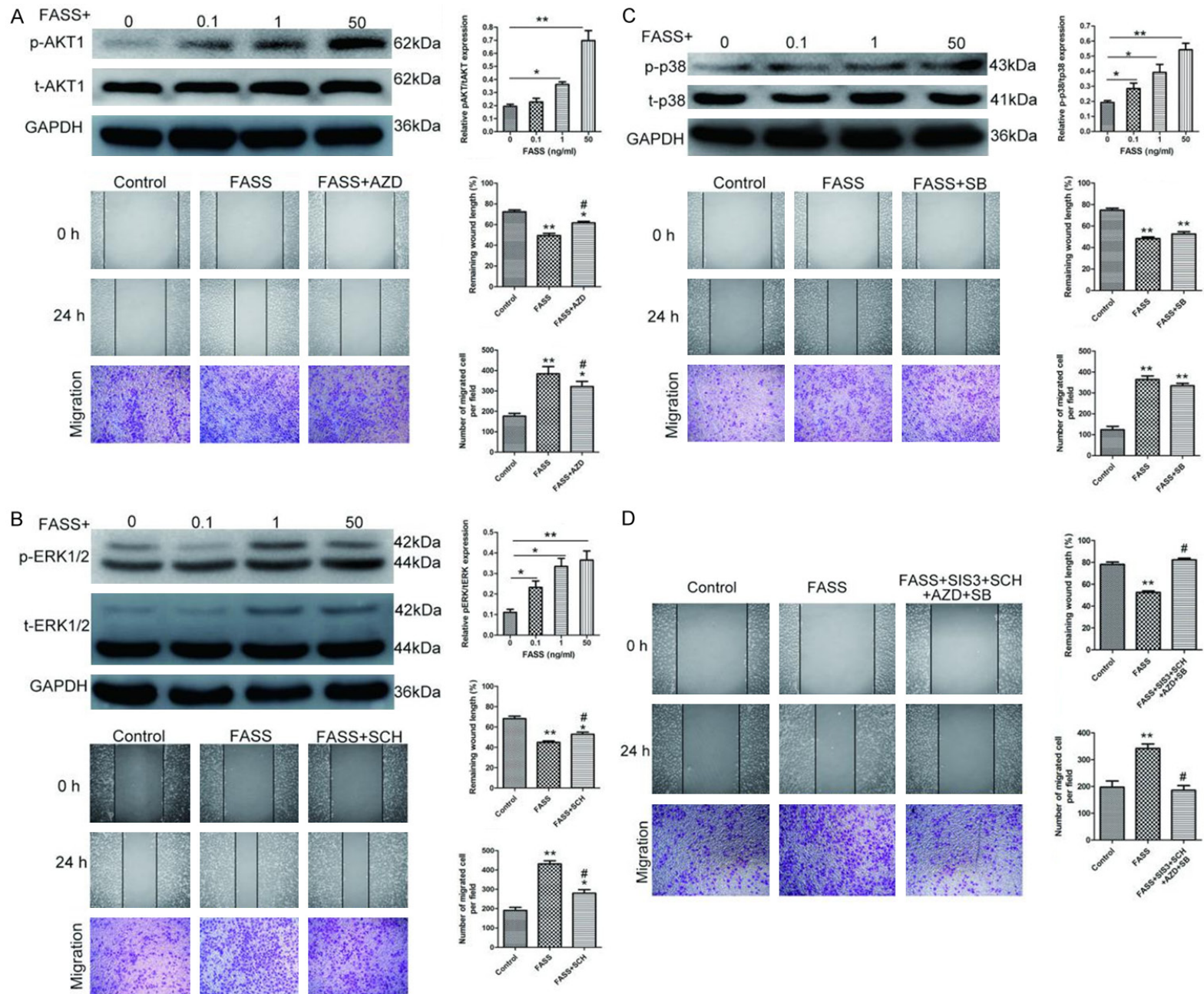


Figure 3. FASSs potentiated TGF-β/Smad3 activity in HUVECs. A. Representative immunofluorescence images showing that FASSs induced Smad3 phosphorylation (p-Smad3) in a dose-dependent manner. Magnification, 200×. B. Representative Western blot showing the significantly increased expression of TGF-β, Smad3, and p-Smad3 in FASSs-treated HUVECs compared with the control. TGF-β expression was also assessed using RT-qPCR. C, D. The scratch and Transwell assays showed that the selective Smad3 inhibitor SIS3 decreased the migratory capacity of FASSs-treated HUVECs. *P<0.05, **P<0.01, compared to the control group. #P<0.05, compared to the FASS group.

Fatty acid extracts promote wound healing



Fatty acid extracts promote wound healing

Figure 4. FASSs increased the expression and phosphorylation of AKT, ERK1/2, and p38 in a dose-dependent manner. Western blot was performed to determine the expression of (A) AKT1 and p-AKT1, (B) ERK1/2 and p-ERK1/2, and (C) p38 and p-p38 in the control (0) and HUVECs treated with different concentrations of FASSs as indicated. Inhibitors AZD5363 (AKT inhibitor), SCH772984 (ERK inhibitor), and SB203580 (p38 MAPK inhibitor) were also used to identify the pathways induced by FASSs. (D) In the scratch and Transwell assays, simultaneous application of these inhibitors completely abolished the effects of FASSs on the activation of these molecules. * $P < 0.05$, ** $P < 0.01$, compared with control. # $P < 0.05$, compared with the FASS group.

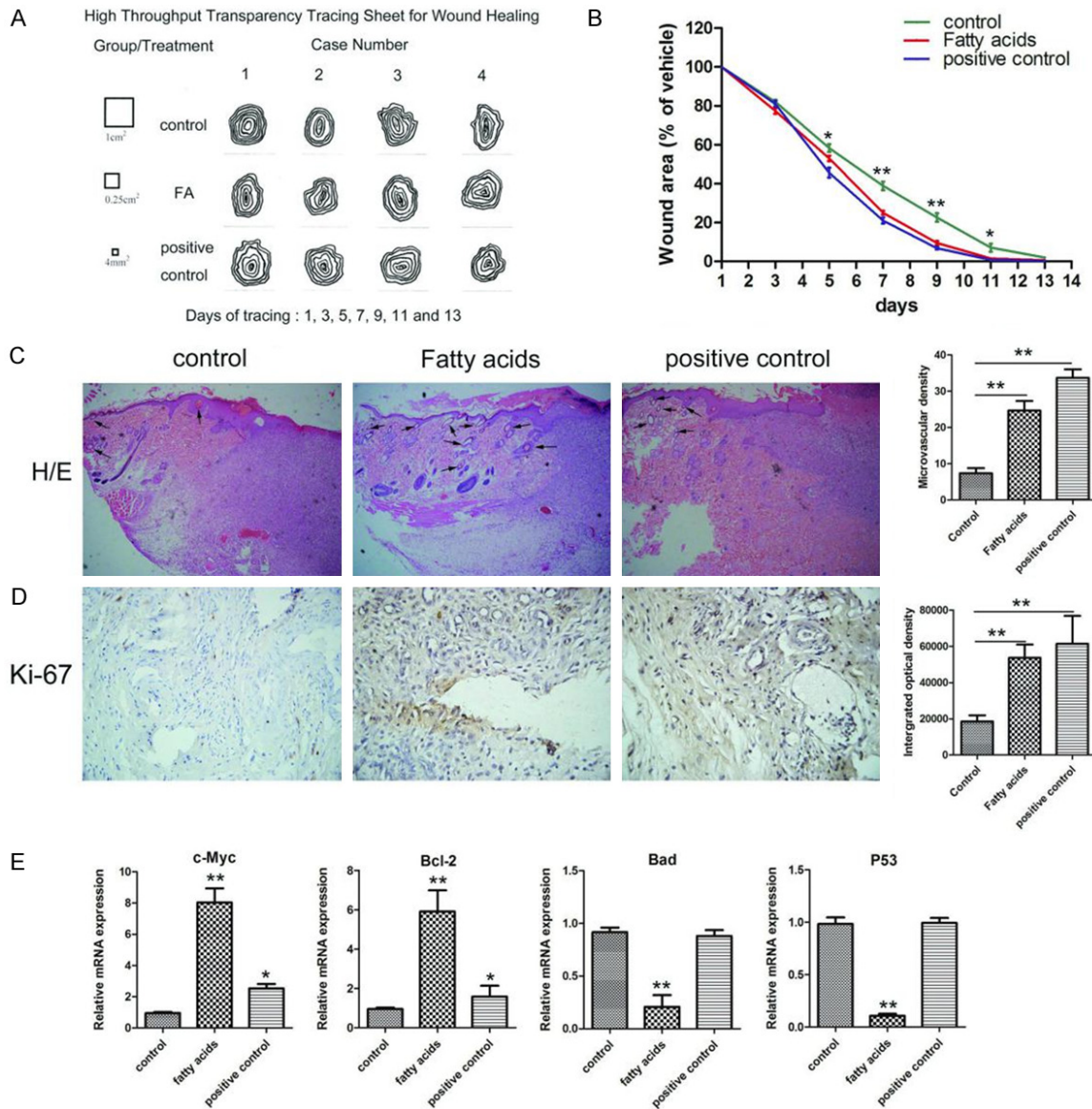


Figure 5. FASSs accelerated cutaneous wound healing by promoting cell proliferation and angiogenesis *in vivo*. A. Transparency tracing was performed on individual wound margins at seven time points (days 1, 3, 5, 7, 9, 11, and 13). B. The average wound healing rates were higher in the FASSs and positive rat groups compared to the control group. C. Representative micrographs of H/E staining of wounds at day 5 showed that the number of microvascular structures was greater in the FASSs and positive groups compared to the control group. Magnification, 100 \times . D. Representative IHC images showing Ki-67 expression in the wound tissues was significantly higher in FASSs and positive groups compared to the control group. Magnification, 200 \times . E. FASSs treatment markedly up-regulated the expression of c-Myc and Bcl-2, which coincided with decreased expression of Bad and p53. * $P < 0.05$, ** $P < 0.01$.

in turn activate downstream targets to augment cell proliferation, migration, and angio-

genesis. The proposed working model is shown in **Figure 6**.

Fatty acid extracts promote wound healing

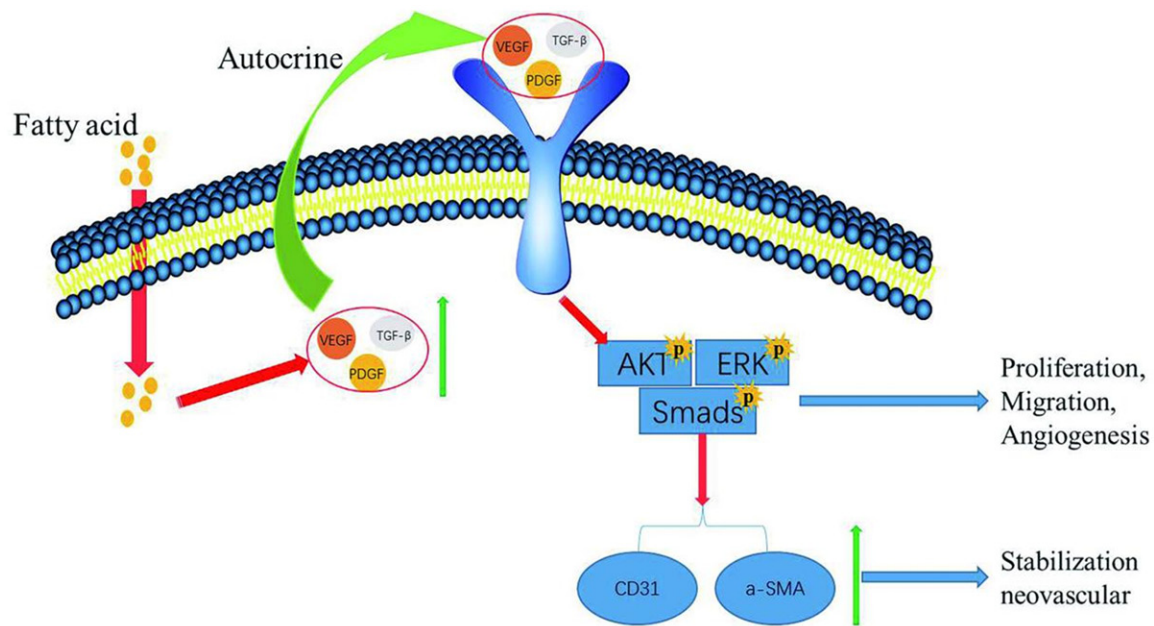


Figure 6. Working model of signaling pathways involved in FASSs-induced HUVEC proliferation, migration, and angiogenesis. FASSs increase the levels of TGF- β , VEGFA, and PDGF. These factors subsequently activate downstream signaling pathways to promote endothelial cell proliferation, migration, and angiogenesis. In addition, FASSs increase the expression of CD31 and α -SMA to stabilize the neovasculature.

In the present study, we chose HUVECs as an *in vitro* system to explore the mechanisms by which FAs promote angiogenesis, and found that FASSs treatment significantly augmented HUVEC proliferation and migration in a dose-dependent manner compared to vehicle treatment. Tube formation was also significantly enhanced by FASSs treatment. Mechanistically, some growth factors (VEGF, PDGF, and TGF- β 1) and their downstream signaling molecules (PI3K/AKT1, ERK1/2, and TGF- β 1/Smad3) that are involved in regulating endothelial cell angiogenesis [11, 12, 14, 15], were significantly increased after FASSs treatment, as evidenced by the increased phosphorylation levels of AKT1 and ERK1/2. Similarly, we revealed that TGF- β 1/p-Smad3, the key proteins that contribute to angiogenesis and cutaneous wound healing [14], were significantly up-regulated by FASSs treatment. Intriguingly, application of specific inhibitors against PI3K/AKT1, ERK1/2, and TGF- β 1/pSmad3 pathways uncovered that FASSs-triggered activation of AKT1 and ERK1/2, but not p-Smad3, played important roles in endothelial cell proliferation and migration. Thus, whether TGF- β 1/pSmad3 is also important in FASSs-facilitated cutaneous wound healing warrants further investigation.

Since mature vasculature supplies nutrients and oxygen to tissues, neovasculature stabilization is crucial for the development of mature neovasculature. The co-expression of CD31 and α -SMA is a well-recognized indicator of neovasculature stabilization and maturity during angiogenesis [22, 31]. In the current study, we found that CD31 and α -SMA expression were markedly increased in HUVECs after FASSs treatment. Moreover, increased α -SMA protein expression in HUVECs was accompanied by well-organized filaments and a fusiform shape, indicating an evolving early time point in EndMT. These findings, taken together, suggest that FASSs promote stabilization and maturation of neovasculature during angiogenesis.

Previously, our group and others showed that FAs promote angiogenesis and improve wound healing *in vivo* [24-26]. Consistent with these previous findings, we found in this study that FAs treatment improved cutaneous wound healing in a rat skin injury model, as evidenced by our observations that the average healing rate of the wounds and the formation of microvascular structures were substantially increased in the FAs-treated group compared to the vehicle group. Our findings are also in accordance with other studies, which showed that

the FAs, such as oleic acid (a MUFA), and their metabolites are mediators of several wound healing events [34-36]. Previous studies revealed that MUFAs produced intracellular messengers to mediate a number of biological activities, including cell proliferation, migration, and angiogenesis [25, 37]. In this study, we found that FAs substantially increased the number of Ki-67+ positive cells in the wound site compared to the control group, which coincided with up-regulated levels of proliferation-related genes (c-Myc and Bcl-2). Although we proposed that one of the mechanisms by which FAs facilitate wound healing *in vivo* is to promote endothelial cell proliferation in the wound regions, double staining with Ki67 and an endothelial cell marker should be examined in future studies to support our conclusion.

In conclusion, we demonstrated that FAs significantly promote endothelial cell proliferation, migration, and angiogenesis, and therefore accelerate cutaneous wound healing. Mechanistically, FAs augment the activity of AKT1, ERK1/2, and TGF- β 1/Smad3 signaling. Our findings expand the understanding of the complex signaling involved in wound healing and provide direct evidence for the clinical application of natural agents that accelerate cutaneous wound healing.

Acknowledgements

This study was supported by National Natural Science Foundation of China (81573734, 817-03673), Liaoning Revitalization Talents Program (XLYC1802014), Liaoning Key Research and Development Planning Project (20172-26015), Distinguished Professor Project of Liaoning Province, Liaoning BaiQianWan Talents Program, Clinical Capability Construction Project for Liaoning Provincial Hospitals (LNCCC-A04-2014), the Dalian outstanding youth science and technology talent project, the Program for the Outstanding innovative Teams of Higher Learning Institution of Liaoning (LR2016064), Basic scientific research projects of colleges and universities (LF2017007, LQ2017038, LQ2017041), the Dalian Medical University Special Grant for Translational Medicine (106061), and the Natural Science Foundation of China of Liaoning Province (20180550087).

Disclosure of conflict of interest

None.

Address correspondence to: Dr. Shouyu Wang, Department of Orthopedics, The First Affiliated Hospital of Dalian Medical University, Institute (College) of Integrative Medicine, Dalian Medical University, No. 222 Zhongshan Road, Dalian 116011, China. Tel: +86-18098876067; Fax: +86-0411-83622844; E-mail: wangshouyu666@126.com; Dr. Yunpeng Diao, College of Pharmacy, Dalian Medical University, Dalian 116044, China. Tel: +86-13700119091; Fax: +86-0411-83622844; E-mail: diaoyu@163.com

References

- [1] Martin P. Wound healing—aiming for perfect skin regeneration. *Science* 1997; 276: 75-81.
- [2] Eming SA, Brachvogel B, Odorisio T and Koch M. Regulation of angiogenesis: wound healing as a model. *Prog Histochem Cytochem* 2007; 42: 115-170.
- [3] Gurtner GC, Werner S, Barrandon Y and Longaker MT. Wound repair and regeneration. *Nature* 2008; 453: 314-321.
- [4] Galiano RD, Tepper OM, Pelo CR, Bhatt KA, Callaghan M, Bastidas N, Bunting S, Steinmetz HG and Gurtner GC. Topical vascular endothelial growth factor accelerates diabetic wound healing through increased angiogenesis and by mobilizing and recruiting bone marrow-derived cells. *Am J Pathol* 2004; 164: 1935-1947.
- [5] Brem H and Tomic-Canic M. Cellular and molecular basis of wound healing in diabetes. *J Clin Invest* 2007; 117: 1219-1222.
- [6] Tonnesen MG, Feng X and Clark RA. Angiogenesis in wound healing. *J Invest Dermatol Symp Proc* 2000; 5: 40-46.
- [7] Rozman P and Bolta Z. Use of platelet growth factors in treating wounds and soft-tissue injuries. *Acta Dermatovenerol Alp Pannonica Adriat* 2007; 16: 156-165.
- [8] Fujiwara M, Muragaki Y and Ooshima A. Up-regulation of transforming growth factor-beta1 and vascular endothelial growth factor in cultured keloid fibroblasts: relevance to angiogenic activity. *Arch Dermatol Res* 2005; 297: 161-169.
- [9] Maharaj AS and D'Amore PA. Roles for VEGF in the adult. *Microvasc Res* 2007; 74: 100-113.
- [10] Johnson KE and Wilgus TA. Vascular endothelial growth factor and angiogenesis in the regulation of cutaneous wound repair. *Adv Wound Care (New Rochelle)* 2014; 3: 647-661.
- [11] Somanath PR, Razorenova OV, Chen J and Byzova TV. Akt1 in endothelial cell and angiogenesis. *Cell Cycle* 2006; 5: 512-518.
- [12] Chen Y, Ramakrishnan DP and Ren B. Regulation of angiogenesis by phospholipid lysophosphatidic acid. *Front Biosci (Landmark Ed)* 2013; 18: 852-861.

Fatty acid extracts promote wound healing

- [13] Matsubayashi Y, Ebisuya M, Honjoh S and Nishida E. ERK activation propagates in epithelial cell sheets and regulates their migration during wound healing. *Curr Biol* 2004; 14: 731-735.
- [14] Barrientos S, Stojadinovic O, Golinko MS, Brem H and Tomic-Canic M. Growth factors and cytokines in wound healing. *Wound Repair Regen* 2008; 16: 585-601.
- [15] Cheng B, Liu HW, Fu XB, Sun TZ and Sheng ZY. Recombinant human platelet-derived growth factor enhanced dermal wound healing by a pathway involving ERK and c-fos in diabetic rats. *J Dermatol Sci* 2007; 45: 193-201.
- [16] Jain RK. Molecular regulation of vessel maturation. *Nat Med* 2003; 9: 685-693.
- [17] Carmeliet P. Mechanisms of angiogenesis and arteriogenesis. *Nat Med* 2000; 6: 389-395.
- [18] Yancopoulos GD, Davis S, Gale NW, Rudge JS, Wiegand SJ and Holash J. Vascular-specific growth factors and blood vessel formation. *Nature* 2000; 407: 242-248.
- [19] Nguyen LL and D'Amore PA. Cellular interactions in vascular growth and differentiation. *Int Rev Cytol* 2001; 204: 1-48.
- [20] Rossant J and Howard L. Signaling pathways in vascular development. *Annu Rev Cell Dev Biol* 2002; 18: 541-573.
- [21] Rousseau S, Houle F and Huot J. Integrating the VEGF signals leading to actin-based motility in vascular endothelial cells. *Trends Cardiovasc Med* 2000; 10: 321-327.
- [22] Lin F, Wang N and Zhang TC. The role of endothelial-mesenchymal transition in development and pathological process. *IUBMB Life* 2012; 64: 717-723.
- [23] Wild T, Rahbarnia A, Kellner M, Sobotka L and Eberlein T. Basics in nutrition and wound healing. *Nutrition* 2010; 26: 862-866.
- [24] Shingel KI, Faure MP, Azoulay L, Roberge C and Deckelbaum RJ. Solid emulsion gel as a vehicle for delivery of polyunsaturated fatty acids: implications for tissue repair, dermal angiogenesis and wound healing. *J Tissue Eng Regen Med* 2008; 2: 383-393.
- [25] Cardoso CR, Souza MA, Ferro EA, Favoreto S Jr and Pena JD. Influence of topical administration of n-3 and n-6 essential and n-9 nonessential fatty acids on the healing of cutaneous wounds. *Wound Repair Regen* 2004; 12: 235-243.
- [26] Zhang Z, Wang S, Diao Y, Zhang J and Lv D. Fatty acid extracts from *Lucilia sericata* larvae promote murine cutaneous wound healing by angiogenic activity. *Lipids Health Dis* 2010; 9: 24.
- [27] Li PN, Li H, Zhong LX, Sun Y, Yu LJ, Wu ML, Zhang LL, Kong QY, Wang SY and Lv DC. Molecular events underlying maggot extract promoted rat in vivo and human in vitro skin wound healing. *Wound Repair Regen* 2015; 23: 65-73.
- [28] Li PN, Li H, Wu ML, Wang SY, Kong QY, Zhang Z, Sun Y, Liu J and Lv DC. A cost-effective transparency-based digital imaging for efficient and accurate wound area measurement. *PLoS One* 2012; 7: e38069.
- [29] Lamalice L, Le Boeuf F and Huot J. Endothelial cell migration during angiogenesis. *Circ Res* 2007; 100: 782-794.
- [30] Valarmathi MT, Davis JM, Yost MJ, Goodwin RL and Potts JD. A three-dimensional model of vasculogenesis. *Biomaterials* 2009; 30: 1098-1112.
- [31] Zhao S, Li L, Wang H, Zhang Y, Cheng X, Zhou N, Rahaman MN, Liu Z, Huang W and Zhang C. Wound dressings composed of copper-doped borate bioactive glass microfibers stimulate angiogenesis and heal full-thickness skin defects in a rodent model. *Biomaterials* 2015; 53: 379-391.
- [32] Medici D. Endothelial-mesenchymal transition in regenerative medicine. *Stem Cells Int* 2016; 2016: 6962801.
- [33] Jun JI and Lau LF. The matricellular protein CCN1 induces fibroblast senescence and restricts fibrosis in cutaneous wound healing. *Nat Cell Biol* 2010; 12: 676-685.
- [34] Sellmayer A, Hrboticky N and Weber PC. Lipids in vascular function. *Lipids* 1999; 34 Suppl: S13-18.
- [35] Claria J. Regulation of cell proliferation and apoptosis by bioactive lipid mediators. *Recent Pat Anticancer Drug Discov* 2006; 1: 369-382.
- [36] Savla U, Appel HJ, Sporn PH and Waters CM. Prostaglandin E(2) regulates wound closure in airway epithelium. *Am J Physiol Lung Cell Mol Physiol* 2001; 280: L421-431.
- [37] Ruthig DJ and Meckling-Gill KA. Both (n-3) and (n-6) fatty acids stimulate wound healing in the rat intestinal epithelial cell line, IEC-6. *J Nutr* 1999; 129: 1791-1798.